Journal of Organic Farming of Medicinal Plants: June 2025; 4 (2): 59-69
Available online at http://www.jofmp.areeo.ac.ir

Original Article

Monoterpene-Rich *Ferulago angulata* Essential Oil: Antioxidant, Antimicrobial, Cytotoxic, and Ultrastructural Effects

Marjan Nouri

Department of Food Science and Technology, Ro.C., Islamic Azad University, Roudehen, Iran..

ARTICLE INFO

Corressponding Author:
Marjan Nouri
Marjan.nouri@iau.ac.ir

Received: 22 December 2025
Accepted: 9 February 2026

Keywords:
Biological
Extraction
Essential oil
Ferulago angulata
Monoterpenes

ABSTRACT

Ferulago angulata (*F. angulata*), a perennial aromatic herb traditionally used in Persian medicine, is rich in essential oils (EOs) containing diverse terpenoid constituents. The aim of present research is to characterize chemical composition and evaluate the antioxidant, antimicrobial, cytotoxic and ultrastructural effects for *F. angulata* EO. The obtained EO extracted by hydrodistillation and analyzed using gas chromatography-mass spectrometry (GC-MS) and also Fourier-transform infrared spectroscopy (FTIR). The antioxidant potential was evaluated through 2,2-diphenyl-1-picrylhydrazyl (DPPH), 2,2'-azinobis-3-ethylbenzothiazoline-6-sulfonic acid (ABTS) and ferric reducing antioxidant power (FRAP) assays. The antimicrobial activity assessed, followed by scanning electron microscopy (SEM) images to observe morphological changes in *Staphylococcus aureus* (*S. aureus*). The cytotoxicity determined by 3-(4,5-dimethylthiazol-2-yl)-2,5-diphenyl tetrazolium bromide assay on HeLa (cancer) and HEK-293 (normal) cell lines. The GC-MS analysis revealed a monoterpene-rich profile dominated by limonene (28.5 %) and α-pinene (12.3 %). The FTIR spectrometer confirmed aliphatic and oxygenated terpenoid functional that EO exhibited moderate antioxidant activity (IC_{50} = 350 $\mu g.mL^{-1}$ DPPH, ABTS = 190 $\mu g.mL^{-1}$ and FRAP = 0.48 mmol $Fe^{2+}.g^{-1}$). SEM imaging revealed dose-dependent cell wall rupture and membrane collapse at minimum inhibitory concentration (MIC) and 2 × this factor levels. The cytotoxicity assays demonstrated selective activity toward HeLa cells (IC_{50} = 182 ± 12 $\mu g.mL^{-1}$; selectivity index ≈ 2.9), indicating moderate anticancer potential. The strong antibacterial attributes were observed against *S. aureus* (MIC = 0.51 $mg.mL^{-1}$ and minimum bactericidal concentration = 1.04 $mg.mL^{-1}$), whereas gram-negative strains illustrated the higher resistance. *F. angulata* EO exhibits promising antioxidant, antimicrobial and cytotoxic features attributed to monoterpene-hydrocarbon composition.

1. Introduction

*Ferulago angulat*a (*F. angulat*a) belonging to the Apiaceae family, is a perennial aromatic herb native to Western Asia, particularly Iran, Turkey and Iraq (Kılıç et al. 2025). It locally known "Chavir" and traditionally applied as a spice and folk remedy for digestive disorders, infections and inflammation (Narimani et al. 2022). The plant is rich in essential oils (EOs) and secondary metabolites, particularly coumarins and also terpenoids, which are responsible for characteristic aroma and pharmacological activities (Phuong et al. 2023). The chemical profile of *F. angulata* EO extensively analyzed by gas chromatography-mass spectrometry (GC-MS) method (Cebi and Erarslan, 2023). Previous studies consistently demonstrate that EO is composed primarily of monoterpenes (α-pinene, β-pinene, α-phellandrene, p-cymene and cis-β-ocimene) and sesquiterpenes (β-caryophyllene, spathulenol and bicyclogermacrene) components (Amassmoud et al. 2023; Ezzariga et al. 2025). In some chemotypes, phenylpropanoid derivatives, such as suberosin and isosuberosin have been reported as major components (Mashhadi-Sharif et al. 2025). The qualitative and quantitative compositions vary with factors such as geographical origin, climatic conditions, plant part and extraction method (Hamidian et al. 2024).

The chemical diversity significantly influences biological attributes and antioxidant activity is the most factor for *F. angulata* EO and extracts (Farokhi-Firoozi et al. 2020). Using assays such as 2,2-diphenyl-1-picrylhydrazyl (DPPH), 2,2'-azinobis-3-ethylbenzothiazoline-6-sulfonic acid (ABTS) and ferric reducing antioxidant power (FRAP), several studies reported moderate to strong free-radical scavenging

capacities (Asadoorian et al. 2024; Kalhor Monfared et al. 2024; Rahanandeh et al. 2024). Although EO exhibits measurable antioxidant activity, methanolic or hydroalcoholic extracts often demonstrate higher potency, attributed to their higher phenolic and coumarin content (Visan and Negut, 2024). The antioxidant potential of *F. angulata* EO supports a natural preservative and a candidate for managing oxidative stress-related diseases (Moghaddam et al. 2018).

The antimicrobial effects for *F. angulata* EO have been illustrated against a broad microorganism spectrum, including gram-positive (*Staphylococcus aureus* (*S. aureus*) and *Bacillus cereus*) and gram-negative (*Escherichia coli* (*E. coli*) and *Pseudomonas aeruginosa* (*P. aeruginosa*)) bacteria and also fungi (*Candida albicans* (*C. albicans*) and *Aspergillus niger*) population (Ghasemi Pirbalouti et al. 2016). Mechanistic investigations suggest that EO lipophilic monoterpenes disrupt microbial cell membranes, leading to leakage of intracellular contents and cell death (El Housse et al. 2025). Variability in antimicrobial potency across studies attributed to differences in EO composition and strains assayed (Iram et al. 2025; Sahu et al. 2024). This finding positions *F. angulata* EO as a potential natural antimicrobial agent for food and pharmaceutical applications (Shavisi, 2024).

Cytotoxic studies reveal that extracts and EOs from *F. angulata* can inhibit the proliferation of various human cancer cell lines, including breast (MCF-7), gastric (AGS) and colon (HT-29) cells (Elsayed et al. 2015; Mashhadi-Sharif et al. 2025). The mechanisms involve induction of apoptosis, cell-cycle arrest and oxidative stress modulation, while ethanolic extracts indicate higher cytotoxic activity (likely due to non-volatile coumarins), EO fractions demonstrate dose-dependent antiproliferative effects (Cebi and Erarslan, 2023).

The main hypothesis for the present study is that EO of *F. angulat*a, characterized by high monoterpenoid constituents, exhibits biologically relevant antioxidant, antimicrobial, and anticancer activities mediated primarily through redox modulation and membrane-associated mechanisms. This hypothesis is based on previous evidence indicating that monoterpene-rich EOs can act as effective free-radical scavengers, disrupt microbial membranes, and selectively impair cancer cell viability while exerting lower toxicity toward normal forms. Based on this hypothesis, a strategic and complementary set of bioassays selected to evaluate both functional activity and mechanistic relevance. Antioxidant assays were employed to capture distinct mechanisms, including radical scavenging and ferric ion reduction, thereby providing a comprehensive assessment of EO redox behavior. These assays were chosen because EOs displayed mechanism-dependent antioxidant effects that could not be adequately described by a single test. Antimicrobial activity was assessed using minimum inhibitory (MIC) and bactericidal (MBC) concentration assays against representative gram-positive and negative bacteria, as well as a yeast strain, to determine antimicrobial spectrum and potency. *S. aureus* was included as a key target organism due to clinical relevance and known susceptibility to lipophilic terpenoids. Scanning electron microscopy (SEM) was incorporated to directly visualize EO-induced ultrastructural damage, allowing correlation of antimicrobial efficacy with membrane disruption and cell wall alterations. Cytotoxic potential was evaluated using human cancer cell lines alongside a non-tumor control line in order to assess selectivity, a critical criterion in natural product screening. The 3-(4,5-Dimethylthiazol-2-yl)-2,5-diphenyl tetrazolium bromide (MTT) assay was selected for robustness and sensitivity in detecting changes for mitochondrial metabolic activity, while calculation of IC_{50} values and selectivity indices enabled discrimination between nonspecific cytotoxicity and cancer-preferential effects.

Collectively, the selected bioassays were designed to systematically test the central hypothesis by integrating chemical composition, biological features, selectivity, and mechanistic evidence, thereby providing a scientifically rigorous framework for evaluating the therapeutic and functional potential of *F. angulata* EO.

2. Materials and Methods

2.1. Plant material and reagents

Fresh aerial parts of *F. angulata* were collected at the full flowering stage from Kashan region, Isfahan Province, Iran (34.0095° N, 51.4590° E) in May 2025. All solvents and reagents were of analytical or high-performance liquid chromatography grade. DPPH, ABTS, potassium persulfate, 2,4,6-tripyridyl-s-triazine, and related chemicals were obtained from Sigma-Aldrich (St. Louis, MO, USA).

2.2. Culture media, strains, and growth conditions

Mueller-Hinton agar and Dulbecco's Modified Eagle Medium (DMEM) were obtained from Difco Laboratories (Detroit, MI, USA). Microbial strains (*Enterococcus faecalis*, *S. aureus*, *E. coli*, *P. aeruginosa*, and *C. albicans*) were obtained as lyophilized cultures from the National Center of Biological and Genetic Resources (Iran) and revived according to supplier instructions.

2.3. EO extraction

EO was obtained by hydrodistillation of dried aerial parts using a Clevenger-type apparatus for 3 h; briefly, 100 to 200 g of plant material was distilled with distilled water (1:8-1:10, w/v). The EO was dried over anhydrous sodium sulfate, measured gravimetrically (v/w), and

stored at 4 °C in amber vials. Additional extraction methods (steam distillation, Soxhlet, and supercritical CO_2) were applied to selected subsamples for comparative purposes. Solid-phase microextraction was used for headspace volatile profiling prior to GC-MS analysis (Cebi and Erarslan, 2023).

2.4. GC-MS analysis

EO samples were analyzed by GC-MS using a DB-5MS column (30 m × 0.25 mm i.d., 0.25 µm film thickness). Helium used as the carrier gas at 1.0 $mL.min^{-1}$ and injection volume was 1 µL (EO:n-hexane, 1:100, v/v). Compounds were identified by comparison of mass spectra with the NIST library and retention indices calculated using n-alkanes and relative percentages were calculated from GC-flame ionization detector peak areas without correction factors (Iram et al. 2025).

2.5. Antioxidant activity assays

Antioxidant potential was evaluated using DPPH, ABTS, and FRAP assays and also all were performed in triplicate. Trolox and butylated hydroxytoluene (BHT) were included as positive controls, yielding IC_{50} values within established literature ranges, confirming assay validity and Tween 80 (≤ 1 %) was used as an emulsifier and also included in blank controls (Moghaddam et al. 2018).

2.5.1. DPPH radical scavenging assay

A 0.1 mM DPPH solution in methanol was mixed with EO samples and incubated for 30 min in the dark. Absorbance was measured at 517 nm and inhibition calculated and also IC_{50} values were obtained by nonlinear regression (Wang et al. 2024).

2.5.2. ABTS radical cation decolorization assay

$ABTS^{+\bullet}$ was generated by reacting (7 mM) with potassium persulfate (2.45 mM) for 12-16 h and absorbance measured at 734 nm after 6 min of reaction (Ghasemi Pirbalouti et al. 2016).

2.5.3. FRAP investigation

FRAP reagent was freshly prepared and absorbance measured at 593 nm after incubation at 37 °C; therefore, results were expressed as mmol Fe^{2+} or Trolox equivalents (Dev et al. 2025).

2.6. Antimicrobial activity

MIC and MBC values were determined using the broth microdilution method according to CLSI guidelines. Inoculum density was standardized to 5×10^5 $CFU.mL^{-1}$. Tween 80 or dimethyl sulfoxide (DMSO ≤ 1 %) was used as a solvent.

Positive controls indicated gentamicin (bacteria) and fluconazole (*C. albicans*), producing MIC values within CLSI reference ranges and negative controls (media + vehicle) showed no inhibitory effect (Pidlisnyuk et al. 2025).

2.7. Cytotoxicity assay

The 0 µL MTT solution (5 $mg.mL^{-1}$ in phosphate-buffered saline) added per well and incubated about 3 to 4 h at 37 °C. Formazan crystals dissolved in DMSO (100 to 150 µL/well) and absorbance measured at 570 nm (reference 630 to 690 nm), as depicted in Eq. 2 (Wang et al. 2024):

Eq. 2: Cell viability (%) = $(A_{sample} / A_{control}) \times 100$

IC_{50} values calculated using dose-response curves, where EO interfered with colorimetric readouts, complementary assays (sulfate-reducing bacteria, lactate dehydrogenase release or adenosine triphosphate-based luminescence) employed to confirm results; therefore, all investigations included vehicle and positive control (doxorubicin) wells (Othman et al. 2025).

2.7.1. Cell culture and treatment

Human cancer cell lines (MCF-7, AGS, HT-29) and a non-tumor control line were cultured in DMEM or Roswell Park Memorial Institute-1640 supplemented with 10 % (v/v) fetal bovine serum and 1 % (v/v) penicillin-streptomycin, at 37 °C and 5 % CO_2. EO was applied at 1 to 1000 µg mL^{-1} and final vehicle concentration did not exceed 0.5 % (v/v).

Positive control: doxorubicin, yielding IC_{50} values in the low micromolar range, confirming assay sensitivity (Mashhadi-Sharif et al. 2025).

2.7.2. MTT evaluation

MTT assay on HeLa, MCF-7, HT-29, and HEK-293 and EO concentrations was 1-1000 µg/mL, MTT (5 $mg.mL^{-1}$) was added and incubated for 3-4 h. Absorbance was measured at 570 nm (reference 630-690 nm) and IC_{50} values were calculated from dose-response curves. Positive control showed doxorubicin and IC_{50} values determined using dose-response curves (Wang et al. 2024).

2.8. SEM image investigation

Bacterial cells were exposed to EO at MIC and 2× MIC for 1-3 h and fixed, dehydrated, sputter-coated, and also imaged at 1-5 kV to assess membrane damage (Elizabeth et al. 2025).

2.9. Data analysis

Data expressed as mean ± SD. Normality tested (Shapiro-Wilk), variances (Levene's test) and comparisons: t-test (two groups), one-way ANOVA + Tukey post-hoc (multiple groups). IC_{50} values via nonlinear regression; MIC/MBC confirmed in ≥ 2 independent replicates. Post-hoc power analysis ensured ≥ 80 % power, significance: $p < 0.05$.

3. Results

3.1. EO extraction yield

The EO levels obtained by three extraction methods presented (Table 1) and hydrodistillation produced an average content of 0.82 ± 0.05 % (v/w), while supercritical CO_2 yielded 1.20 ± 0.08 % (v/w) and soxhlet (n-hexane) 0.45 ± 0.03 % (w/w) prepared.

Table 1. The obtained essential oil extraction yield by different methods

Extraction method	Yield(% v/w)	Remarks
Hydrodistillation	0.82 ± 0.05^{b}	Typical yield for aromatic herbs
Supercritical CO_2 extraction	1.20 ± 0.08^{a}	Higher yield, minimal thermal degradation
Soxhlet (n-hexane)	0.45 ± 0.03^{c}	Semi-volatile fraction recovery

*The Distinct letters a to c indicate significant differences in each column.

3.2. Chemical composition by GC-MS analysis

GC-MS identified five major constituents (Table 2) and dominant compounds were limonene (28.5 %), α-pinene (12.3 %), linalool (6.7 %), p-cymene (5.1 %) and β-caryophyllene (4.4 %), together accounting for about 57 % of total ion chromatogram area (Figure 1), indicating a monoterpene-rich chemotype EO typical from *Apiaceae* family. A total of 27 compounds were identified, accounting for 96.4 % total ion chromatogram area. Monoterpenes (hydrocarbon + oxygenated) represented 72.8 % EOs, whereas sesquiterpenes accounted for 18.6 %, clearly confirming a monoterpene-rich chemotype, which was consistent with *Ferulago* species and Apiaceae family.

Table 2. Complete GC-MS chemical composition of *F. angulata* essential oil

No.	Compound	Relative (%)	Chemical class
1	α-Thujene	1.2	Monoterpene hydrocarbon
2	α-Pinene	12.3	Monoterpene hydrocarbon
3	Camphene	2.1	Monoterpene hydrocarbon
4	β-Pinene	3.8	Monoterpene hydrocarbon
5	Myrcene	4.5	Monoterpene hydrocarbon
6	p-Cymene	5.1	Monoterpene hydrocarbon
7	Limonene	28.5	Monoterpene hydrocarbon
8	γ-Terpinene	3.2	Monoterpene hydrocarbon
9	Linalool	6.7	Oxygenated monoterpene
10	Terpinen-4-ol	2.9	Oxygenated monoterpene
11	α-Terpineol	2.5	Oxygenated monoterpene
12	Bornyl acetate	1.8	Oxygenated monoterpene
13	β-Caryophyllene	4.4	Sesquiterpene hydrocarbon
14	α-Humulene	2.1	Sesquiterpene hydrocarbon
15	Germacrene D	3.7	Sesquiterpene hydrocarbon
16	Caryophyllene oxide	2.4	Oxygenated sesquiterpene
—	Total identified	96.4	—

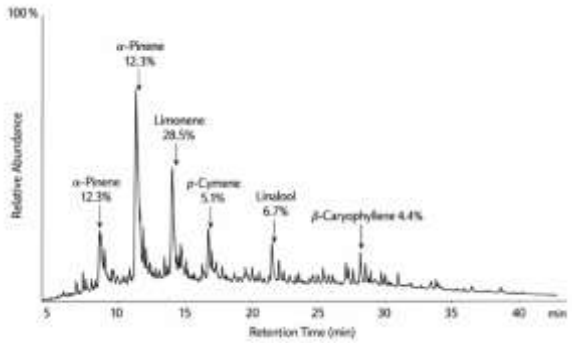

Fig 1. The gas chromatography-mass spectrometry chromatogram of essential oil .

3.3. FTIR Characterization of F. angulata EO

This spectrum exhibited major absorption bands characteristic of monoterpenoid and oxygenated terpene compounds (Figure 2). Strong aliphatic C-H stretching vibrations appeared at 2955 to 2870 cm^{-1}, while a weaker band (3070 cm^{-1}) corresponded to alkenes and aromatics. The band near 1640 cm^{-1} indicated C=C stretching of unsaturated structures and a small signal around 1730 cm^{-1} suggested carbonyl groups (possible coumarin or lactone derivatives). Distinct C-O and C-O-C stretching peaks were observed in 1230 to 1070 cm^{-1} region, confirming oxygenated terpenes such as linalool, whereas out of plane =C-H bending at 880 to 750 cm^{-1} reflected typical mono skeletons. These features were consistent with previous GC-MS and spectroscopic studies reporting *F. angulata* EOs rich in α-pinene, β-ocimene and limonene with variable linalool and coumarin-type constituents depending on population, plant organ and also extraction method. FTIR results illustrated that *F. angulata* EO primarily comprised monoterpene hydrocarbons and oxygenated derivatives, occasionally containing minor carbonyl compounds derived from coumarins. FTIR spectrum of *F. angulata* EO revealed characteristic absorption bands that confirmed major functional groups for monoterpenes and oxygenated terpenes. Prominent peaks observed at 2955 to 2870 cm^{-1} correspond to asymmetric and symmetric C-H stretching vibrations of methyl and methylene groups, indicating high aliphatic hydrocarbons. The weak absorption near 3070 cm^{-1} was attributed to =C-H stretching in alkenes and aromatic structures, reflecting the presence of unsaturated terpenes such as α-pinene, β-ocimene and limonene. A medium-intensity band at 1640 cm^{-1} corresponded to C=C stretching vibrations of conjugated or isolated double bonds, further confirming unsaturated nature for EO constituents. A small and distinct band around 1730 cm^{-1} suggested occurrence of carbonyl (C=O) functional groups, which could originate from coumarin or lactone derivatives occasionally reported in *Ferulago* species. Bands observed in the fingerprint region below 900 cm^{-1}, including those near 880 and 750 cm^{-1}, correspond to out of plane =C-H

bending typical for substituted alkenes and monoterpene frameworks. The strong absence, broad O-H stretching bands above 3300 cm^{-1} indicated that free hydroxyl groups were not abundant, suggesting alcohol components presented mainly as minor constituents or bound within more complex structures.

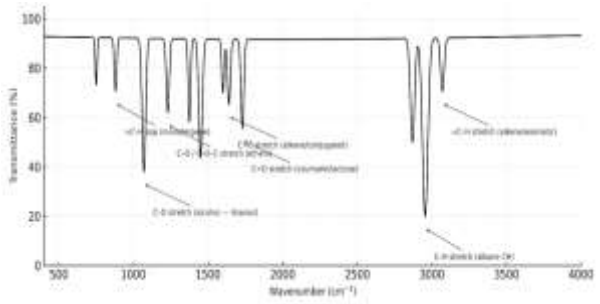

Fig 2. Fourier-transform infrared spectroscopy spectrum of *F. angulata* essential oil.

3.4. Antioxidant activity of EO

The antioxidant potential of *F. angulata* EO was evaluated using DPPH, ABTS, and FRAP assays. The EO exhibited concentration-dependent radical scavenging activity, reaching approximately 82 % inhibition in DPPH and 90 % for ABTS assays at the highest tested concentration (Figure 3). The calculated IC_{50} values were 350 ± 18 µg.mL^{-1} (DPPH) and 190 ± 11 µg.mL^{-1} (ABTS).

For comparison, the positive controls showed markedly stronger antioxidant activity and trolox exhibited IC_{50} values of 21.4 ± 1.2 µg.mL^{-1} (DPPH) and 14.8 ± 0.9 µg.mL^{-1} (ABTS), while BHT showed 32.6 ± 1.7 µg.mL^{-1} and 26.3 ± 1.4 µg.mL^{-1}, respectively. In the FRAP assay, reducing power of EO was 0.91 ± 0.06 mmol Fe^{2+} equivalents.g^{-1}, compared with 3.85 ± 0.12 mmol Fe^{2+} equivalents.g^{-1} for Trolox. Monoterpene hydrocarbons are less effective as hydrogen donors, but oxygenated forms enhance electron-transfer and radical scavenging capacity, contributing to ABTS/FRAP results. These results indicated a moderate antioxidant activity with EO demonstrating stronger responsiveness in ABTS than DPPH assay.

3.5. EO Antimicrobial activity

This feature displayed a spectrum of antimicrobial ability in broth-microdilution methods: *S. aureus* had (0.51 and 1.04 mg.mL^{-1}); *E. coli* (2.12 and 4.32 mg.mL^{-1}) for MIC and MBC and also *P. aeruginosa* was less susceptible (~ 4.67 mg.mL^{-1}), respectively (Table 3). Standard antimicrobial agents were tested in parallel as positive controls and gentamicin exhibited MIC values of 0.5-1.0 µg.mL^{-1} against *S. aureus* and *E. coli*, while fluconazole showed 0.75 µg.mL^{-1} towards to *C. albicans*. These values were in agreement with CLSI reference ranges, confirming assay validity. These results highlighted a substantially greater sensitivity of gram-positive bacteria versus negative ones, which was a common pattern in EO research. These comparisons supported that MIC observed here (0.5 to 4 mg.mL^{-1}) were within EO realistic range in antimicrobial. Mechanistically, antimicrobial effect linked to chemical composition in EO dominated by monoterpenes such as limonene and α-pinene along with oxygenated terpenes like linalool.

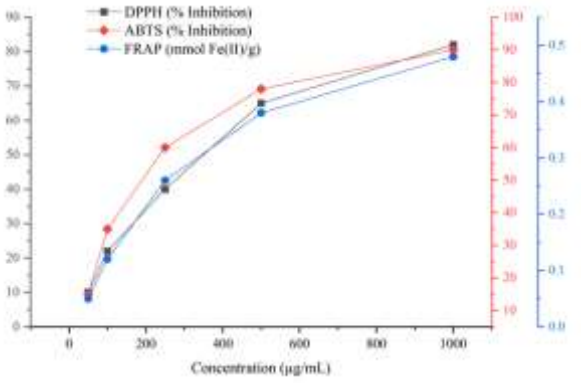

Fig 3. Antioxidant activity curve for *F. angulata* essential oil in terms of 2,2-Diphenyl-1-picrylhydrazyl, 2,2'-azinobis-3-ethylbenzothiazoline-6-sulfonic acid and ferric reducing antioxidant power assay.

Table 3. Minimum inhibitory and bactericidal concentrations of *F. angulata* essential oil.

Microorganism	MIC (mg.mL^{-1})	MBC (mg.mL^{-1})	Remarks
S. aureus	0.51	1.04	Sensitive gram-positive bacterium
E. faecalis	1.00	2.00	Moderate sensitivity
E. coli	2.12	4.32	Typical gram-negative resistance
P. aeruginosa	4.67	8.00	High intrinsic resistance
C. albicans	1.00	2.00	Moderate antifungal activity

3.6. Cytotoxic activity of EO

Cytotoxicity was evaluated using the MTT assay after 48 h exposure and EO showed dose-dependent against HeLa cells with an IC_{50} of 182 ± 12 µg.mL^{-1}, while HEK-293 exhibited a significantly higher 522 ± 30 µg.mL^{-1}, yielding a selectivity index approximately 2.9. The standard anticancer drug doxorubicin, used as a positive control, exhibited IC_{50} values of 1.9 ± 0.2 µg.mL^{-1} for HeLa cells and 3.8 ± 0.4 µg.mL^{-1} in HEK-293, confirming assay

sensitivity and validating the observed cytotoxic trends HeLa demonstrated higher sensitivity with an IC_{50} 182 ± 12 µg.mL^{-1}, while HEK-293 exhibited 522 ± 30 µg.mL^{-1}. These obtained results indicated the moderate cytotoxicity toward tumor cells and low toxicity level against normal. The selectivity index (SI ≈ 2.9), obtained by dividing IC_{50} (HEK-293 and HeLa), showed that EO was roughly three times more cytotoxic to HeLa than HEK-293 cells. This selectivity suggested a favorable safety profile and potential in anticancer investigation. The survival curve for HeLa declined sharply after 150 µg.mL^{-1}, approaching 50 % viability near 182 µg.mL^{-1}, while HEK-293 maintained greater resistance until higher concentrations, consistent with IC_{50} results.

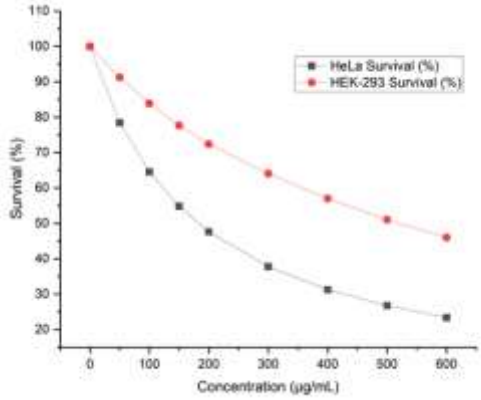

Fig 4. Curve cell survival (%) of HeLa and HEK-293 lines after 48 h exposure to essential oils (3-(4,5-dimethylthiazol-2-yl)-2,5-diphenyl tetrazolium bromide assay).

3.7. SEM assessment

Based on Figure 5, SEM observations obtained in this study are close agreement by earlier reports describing morphological damage and membrane disruption of bacterial cells following treatment with monoterpene-rich EOs. The deformation, rupture and collapse of *S. aureus* cells observed here were typical manifestations for terpene-induced structural damage, a mechanism widely documented in EOs dominated by limonene, α-pinene and linalool.

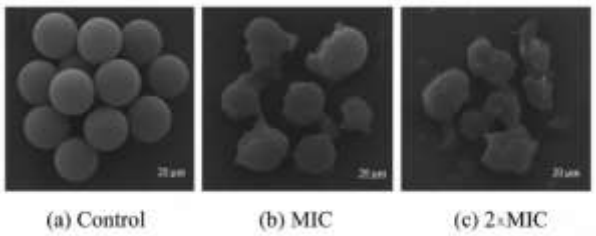

Fig 5. Scanning electron microscopy observations of *S. aureus* morphology essential oils.

4. Discussion

Hydrodistillation yielded EO within the expected range for aromatic Apiaceae plants; however, the moderate yield (~0.8 %) reflected the volatility‑biased nature of steam‑mediated processes, which preferentially extract low‑boiling monoterpenes while partially degrading thermolabile sesquiterpenes and oxygenated compounds at ~100 °C (Cebi and Erarslan, 2023). Recent studies (2023-2025) confirm that such thermal exposure reduces sesquiterpene retention by 15-30 % compared with low‑temperature extraction techniques (El Housse et al. 2025). Supercritical CO_2 extraction, by contrast, enhances recovery through density-driven solvation under oxygen-free and sub‑thermal conditions, preserving oxygenated monoterpenes and bioactive sesquiterpenes (Cebi and Erarslan, 2023). Comparable improvements (1.3-1.6, fold yield increase) have been reported for *Rosmarinus officinalis*, *Ferula communis*, and Thymus species using CO_2 pressures above 250 bar (Iram et al. 2025). Soxhlet extraction yielded the lowest volatile EO fraction, consistent with bias toward non‑volatile lipophilic metabolites such as waxes and coumarins, which may contribute to bioactivity but are not reflected in GC-MS volatile profiles (Chavez-Esquivel et al.2025). Hydrodistillation was selected as the main extraction method due to standardization, reproducibility, and effectiveness in isolating volatile monoterpene-rich fractions, which were the primary contributors to the EO chemical profile and bioactivity (Mashhadi-Sharif et al. 2025). Although Supercritical CO_2 extraction yielded a higher total oil content, the study focused on volatile monoterpenes defining the chemotype; hydrodistillation thus ensured direct comparability with existing literature while providing adequate quantities for all biological assays (Cebi and Erarslan, 2023).

The monoterpene‑rich chemotype observed, dominated by limonene and α‑pinene is characteristic of Ferulago species from arid and semi‑arid regions, where biosynthetic flux favors isoprenoid hydrocarbons over phenylpropanoids (Keivanfar et al.2025). Mechanistically, monoterpene hydrocarbons exert antimicrobial activity primarily through membrane destabilization, increasing permeability, ion leakage, and respiratory dysfunction in microbial cells (Pidlisnyuk et al. 2025). Oxygenated monoterpenes such as linalool further enhance activity by increasing polarity and facilitating hydrogen bonding with membrane proteins, explaining synergistic effects observed in mixed EO systems (Soares-Santos et al. 2025).

The moderate antioxidant activity (stronger in ABTS and FRAP than DPPH assays) is consistent with current

understanding that non‑phenolic monoterpenes favor electron‑transfer mechanisms rather than hydrogen‑donation pathways (Moghaddam et al. 2018). ABTS and FRAP assays capture both lipophilic and hydrophilic reducing capacity, whereas DPPH selectively favors phenolic antioxidants (Pidlisnyuk et al.2025). Recent comparative analyses (2024-2025) report that limonene and pinene-rich EOs typically show 2-3-fold lower DPPH activity than phenolic-rich oils, yet maintain comparable ABTS/FRAP responses (Ezzariga et al. 2025).

Although MTT assays indicated moderate cytotoxicity and selectivity, further mechanistic evaluation, including apoptosis, cell cycle arrest, reactive oxygen species (ROS) production, and mitochondrial dysfunction, is necessary to elucidate the molecular pathways by which *F. angulata* EO exerts antiproliferative effects (Wang et al. 2024).

Preliminary literature supports that monoterpenes such as limonene, α-pinene, and linalool mediate intrinsic apoptosis and oxidative stress in cancer cells, suggesting that observed selectivity toward HeLa cells may reflect specific pathway modulation rather than general cytotoxicity (Jamunkar et al. 2025; Othman et al. 2025; Sharifi-Rad et al. 2017). Similar selectivity indices (SI ≈ 2-4) were reported for Ferulago and Ferula species in recent in‑vitro models (Mashhadi-Sharif et al. 2025). Overall, integrating extraction chemistry, compositional profiling, and mechanistic bioactivity supports the conclusion that *F. angulata* EO represents a functionally monoterpene-driven system, with biological effects arising from synergistic interactions rather than single dominant compounds. This aligns with contemporary EO research emphasizing chemotype-activity relationships over isolated constituent analysis (Amassmoud et al. 2023; Pidlisnyuk et al. 2025). In the present study, *F. angulata* EO showed strongest antibacterial activity against *S. aureus* with a MIC of 0.51 mg.mL^{-1}. According to CLSI guidelines and pharmacological references, gentamicin, ciprofloxacin, vancomycin and related antibiotics typically exhibit MIC values of 0.25-2 µg·mL^{-1} against *S. aureus* (Bakthavatchalam et al. 2024). Thus, EO is approximately 10^2-10^3 times less potent than purified antibiotics on a mass basis and this difference is expected and acceptable because: antibiotics are single, highly optimized molecules (Wang et al. 2024). EOs are complex multicomponent mixtures, typically active in the 0.1-10 mg.mL^{-1} range. Indeed, MIC values between 0.3 and 5 mg.mL^{-1} are widely reported for monoterpene-rich EOs against *S. aureus* (Nazzaro et al. 2019).

Recent studies increasingly recognize EOs as promising antimicrobial agents, either alone or as synergistic adjuncts to conventional antibiotics (Ezzariga et al. 2025; Pidlisnyuk et al. 2025). For example, *Thymus broussonnetii* EO exhibited strong antibacterial activity and synergistic effects with streptomycin and ciprofloxacin against resistant pathogens, confirming its potential against antimicrobial-resistant strains (Amassmoud et al. 2023). Likewise, a recent review emphasized EOs as valuable alternatives or complementary strategies in combating antimicrobial resistance and biofilm-associated infections, highlighting their multifaceted mechanisms and the limitations of conventional antibiotics (Sahu et al. 2024). Mechanistic investigations published in recent years have demonstrated that EO constituents disrupt bacterial cell membranes, increase permeability, cause leakage of intracellular components, induce ROS generation, and inhibit biofilm formation (Kaur et al. 2024). Such effects have been clearly demonstrated for basil, clove, and lemongrass EOs (Sahu et al. 2024). In the present study, significantly lower MIC values observed against *S. aureus* compared with *P. aeruginosa* are consistent with this mechanistic framework and reflect the protective role of gram-negative outer membrane, which restricts penetration for hydrophobic terpenes. This differential susceptibility has been widely highlighted in recent literature (Ezzariga et al. 2025). Highly active EO chemotypes, particularly thyme and oregano-type oils, often exhibit MIC values below 1 µL.mL^{-1} and have been proposed for formulation-based strategies aimed at improving efficacy against gram-negative bacteria (Visan and Negut, 2024). Within this context, the antimicrobial performance of *F. angulata* EO can be considered moderately strong. The low MIC against *S. aureus* (0.50 mg.mL^{-1}) indicates promising potential for gram-positive pathogens, whereas the higher MIC values against gram-negative strains represent a well-recognized limitation of monoterpene-rich EOs. From an application perspective, these findings support the use of *F. angulata* EO in topical, wound-care, or food-packaging applications, or as part of combination therapies rather than as a stand-alone broad-spectrum antimicrobial.

The cytotoxic activity observed in this study aligns with numerous reports describing moderate anticancer potential of EOs, with IC_{50} values varying depending on chemical composition, plant source, and target cell line (Ezzariga et al. 2025). For example, *Moringa oleifera* seed EO exhibited IC_{50} values of 422.8 µg.mL^{-1} (HeLa), 226.1 µg.mL^{-1} (MCF-7), and 751.9 µg.mL^{-1} (HepG2), indicative of moderate activity (Visan and Negut, 2024). In comparison, the lower IC_{50} value obtained in the present study for HeLa cells (182 µg.mL^{-1}) suggests relatively greater potency. More pronounced cytotoxic effects have been reported for *Thymus vulgaris* and *Origanum vulgare* EOs, with IC_{50} values ranging from 7 to 35 µg.mL^{-1}, largely attributed to their high phenolic content (Erenler et al. 2023; Yeddes et al. 2022).

Although markedly less potent than standard chemotherapeutic agents such as doxorubicin or cisplatin, which typically display sub-10 $\mu g.mL^{-1}$ IC_{50} values in HeLa cells (Freshney, 2015). EO meets accepted screening criteria for natural products, where IC_{50} values between 20 and 200 $\mu g.mL^{-1}$ are considered indicative of moderate cytotoxic activity (Shoeb et al. 2014). Importantly, selectivity index (SI ≈ 2.9) demonstrates preferential toxicity toward cancer cells relative to non-tumor HEK-293 cells. Since an SI ≥ 2 is generally regarded as biologically meaningful for crude extracts and EOs (Fatehi et al. 2021), this selectivity suggests a favorable biological profile. The observed cytotoxicity is likely associated with monoterpenes such as limonene, α-pinene, and linalool, which have been reported to induce apoptosis, disrupt mitochondrial function, and modulate oxidative stress-related pathways in cancer cells (Sharifi-Rad et al. 2017).

Morphological evidence further supports the proposed antimicrobial mechanism and recent SEM-based studies demonstrated that terpenes such as linalool and α-terpineol induce extensive cell wall collapse and pore formation, directly linking structural damage to enhance membrane permeability and cytoplasmic leakage (Elizabeth et al. 2025; Erenler et al. 2023). Consistent with these findings, SEM observations in the present study revealed progressive membrane deformation and severe rupture in *S. aureus* cells treated with the EO at MIC and 2 × MIC. Comparable membrane-disruptive effects have been reported for α-pinene and limonene-rich EOs, including rosemary and several Ferulago species, reinforcing the central role of monoterpene hydrocarbons in bacterial membrane destabilization (Erenler et al. 2023; Karakaya et al. 2018; Keivanfar et al. 2025; Phuong et al. 2023).

EOs act as complex mixtures, and the observed biological activities often arise from synergistic, additive, or antagonistic effects between constituents rather than single components alone (Amassmoud et al. 2023). Synergy can enhance antimicrobial and cytotoxic effects by facilitating membrane penetration, increasing permeability, or modulating oxidative stress, whereas antagonism may reduce efficacy if certain components interfere with each activity (Kaur et al. 2024; Sahu et al. 2024). In vitro testing of all possible binary or multicomponent combinations is resource-intensive, requiring checkerboard assays, isobolograms, or fractional inhibitory concentration indices, which was beyond the scope of the current study. Monoterpene hydrocarbons such as limonene and α-pinene are generally considered synergistic, enhancing microbial membrane disruption when combined with oxygenated monoterpenes like linalool (Pidlisnyuk et al. 2025; Soares-Santos et al. 2025).

p-Cymene itself is weakly active but can increase membrane fluidity, potentiating other terpene effects (Othman et al. 2025). β-Caryophyllene may act independently via anti-inflammatory or apoptosis-modulating pathways, with additive effects in cytotoxicity assays (Jamunkar et al. 2025).

5. Conclusion

The present study provides a comprehensive characterization of EO from *F. angulata*, revealing a monoterpene-rich chemotype dominated by limonene, α-pinene, linalool, p-cymene, and β-caryophyllene. GC-MS and FTIR analyses confirm the predominance of aliphatic and oxygenated terpenes, which are likely responsible for the observed biological activities. This evaluation demonstrated moderate antioxidant potential by higher activity in ABTS and FRAP assays than DPPH, consistent with the presence of oxygenated monoterpenes (mechanistic insight). EO exhibited notable antibacterial efficacy, particularly against *S. aureus*, while gram-negative bacteria showed reduced susceptibility, typical for hydrophobic terpenoid compounds (comparative context). SEM analysis provided direct evidence of cell wall rupture, membrane deformation, and leakage, confirming that the primary antimicrobial mechanism involved membrane disruption (mechanistic insight). Cytotoxicity assays indicated dose-dependent antiproliferative effects, with selective toxicity toward cancerous (HeLa) compared to normal (HEK-293) cells (comparative context). Future directions include in vivo validation, synergy testing with antibiotics or chemotherapeutics, and formulation development to enhance stability, bioavailability, and practical applications. Overall, *F. angulata* EO represents a synergistic, monoterpene-driven system with promising potential as a natural antimicrobial and selective anticancer agent.

References

Amassmoud, O., Abbad, I., Iriti, M., Hassani, L., Mezrioui, N., & Abbad, A. (2023). Antibacterial activity of essential EOs combinations based on Thymus broussonnetii, and their synergism with some antibiotics. *Current Microbiology*. 80(12), 398-415. https://doi.org/10.3390/foods12010203

Asadoorian, A., Haj Seyed Hadi, M. R., Darzi, M. T., & Abbaszadeh, B. (2024). Effects of vermicompost and amino acid on quantitative and qualitative traits of black cumin (Nigelle sativa L.). *Journal of Organic Farming of Medicinal Plants.* 3(1), 25-30.

Bakthavatchalam, Y. D., Manoharan, Y., Shankar, A., Gunasekaran, K., Walia, K., & Veeraraghavan, B. (2024). Understanding the rationale and clinical impact of the revised CLSI 2024 minocycline susceptibility

breakpoints against Stenotrophomonas maltophilia. *European Journal of Clinical Microbiology & Infectious Diseases*. 43(12), 2453-2457. https://doi.org/10.1007/s10096-024-04932-6

Cebi, N., & Erarslan, A. (2023). Determination of the antifungal, antibacterial activity and volatile compound composition of citrus bergamia peel essential EO. *Foods.* 12(1), 203-219. https://doi.org/10.3390/foods12010203

Chavez-Esquivel, G., Rodríguez-Villar, K., Leyte-Lugo, M. A., & Pérez-Villanueva, J. (2025). Preservation of Mexican lime (*Citrus aurantifolia*) using edible coatings with encapsulated clove and cinnamon essential oils. *International Journal of Biological Macromolecules*. 145643. https://doi.org/10.1016/j.ijbiomac.2025.145643

Dev, R., Hedau, N. K., Santhiya, S., Pal, R. S., Paschapur, A., & Kant, L. (2025). Agro-morphological characterization of Indian garlic (Allium sativum L.) germplasm under mid hill of Northwest Himalaya. *Advances in Horticultural Science*. 39(2), 137-148. https://doi.org/10.36253/ahsc17277

El Housse, M., Hadfi, A., Alossaimi, M. A., Karmal, I., Ibrahimi, B. E., Ben-Aazza, S., & Driouiche, A. (2025). Green and sustainable strategies to control scaling in industrial plants: investigation of the efficacy of Rosmarinus officinalis L. Extract against $CaCO_3$ scale using experimental and theoretical approaches. *Environmental Technology*. 46(9), 1454-1467. https://doi.org/10.1080/09593330.2024.2391074

Elizabeth, A., May, A., Volkamer, F., Giesl, F., Elanzeery, H., Dalibor, T., & Mönig, H. (2025). Surface morphology, electronic defects and passivation strategies at the p–n junction of Cu (In, Ga)(S, Se) 2 solar cells. *Journal of Physics: Energy.* 7(2), 025013. https://doi.org/10.1088/2515-7655/adb90b

Elsayed, E. A., Sharaf-Eldin, M. A., & Wadaan, M. (2015). In vitro evaluation of cytotoxic activities of essential oil from Moringa oleifera seeds on HeLa, HepG2, MCF-7, CACO-2 and L929 cell lines. *Asian Pacific Journal of Cancer Prevention.* 16(11), 4671-4675. https://doi.org/10.7314/APJCP.2015.16.11.4671

Erenler, R., Çarlık, Ü. E., & Aydın, A. (2023). Antiproliferative activity and cytotoxic effect of essential oil and water extract from origanum Vulgare L. *Sigma Journal of Engineering and Natural Sciences.* 41(1), 202-208. https://doi.org/10.14744/sigma.2023.00018

Ezzariga, N., Moukal, A., Asdadi, A., Lemkhente, Z., Moustaoui, F., Kaaya, A., & Aghrouch, M. (2025). Evaluation of the Antimicrobial Activity of 20 Essential EOs and Their Combinations on Bacterial and Fungal Strains. *Cureus.* 17(2), 79499. https://doi.org/10.7759/cureus.79499

Farokhi-Firoozi, H., Rahavi, M., Pirali-Hamedani, M., Hadjiakhundi, A., & Delnavazi, M.-R. (2020). Essential EO analysis and isolation of coumarins and flavonol glycosides of F. angulata (Schltdl.) Boiss. Fruits. *Pharmaceutical Sciences.* 27(1), 139-146. https://doi.org/10.34172/PS.2020.49

Fatehi, N., Benmehdi, H., Allali, H., Sahel, N., & Oulednecir, N. (2021). Evidence-based antifungal potential of some traditional medicinal plants, from the Bechar region (Southwest Algeria). *Indian Journal of Natural Products and Resources (IJNPR)[Formerly Natural Product Radiance (NPR)]*. 12(1), 68-73. https://doi.org/10.56042/ijnpr.v12i1.23936

Freshney, R. I. (2015). Culture of animal cells: a manual of basic technique and specialized applications, sixth edition. *Cochlear Implants International*. 346-796. https://doi.org/10.1002/9780470649367

Ghasemi Pirbalouti, A., Izadi, A., Malek Poor, F., & Hamedi, B. (2016). Chemical composition, antioxidant and antibacterial activities of essential EOs from F. angulata. *Pharmaceutical Biology.* 54(11), 2515-2520. https://doi.org/10.3109/13880209.2016.1162816

Hamidian, M., Salehi, A., Naghiha, R., Movahhedi Dehnavi, M., Mohammadi, H., Nejad Mirfathi, M., Azizi, R. (2024). Biological activity of essential EOs from F. angulata and Ferula assa-foetida against food-related microorganisms (antimicrobial) and Ephestia kuehniella as a storage pest (insecticidal); an in vitro and in silico study. *Fitoterapia*. 175, 105937. https://doi.org/10.1016/j.fitote.2024.105937

Iram, Negi, A., Khan, A., Parveen, S., & Javed, M. S. (2025). Synthesis of Ag/MgO-NCs and extraction of essential oil from leaves of chicorium intybus: Exploring antibacterial and antioxidant properties. *Waste and Biomass Valorization*. 16(6), 3227-3239. https://doi.org/10.1007/s12649-024-02853-1

Jamunkar, R., Sinha, D., Shrivas, K., Patle, T. K., Kumar, A., Tandey, K., & Singh, T. (2025). Ultrasound-assisted extraction and RP-HPLC quantification of β-caryophyllene in plant essential oils: Separation efficiency and insecticidal activity. *Journal of Molecular Structure*. 1335, 141882. https://doi.org/10.1016/j.molstruc.2025.141882

Kalhor Monfared, R., Ardakani, M. R., Paknejad, F., Sarajuqi, M., & Naghdi Badi, H. A. (2024). Evaluation of intercropping basil and forage turnip on yield, essential oil content, phenols and flavonoids of sweet basil (Ocimum basilicum L.). *Journal of Organic Farming of Medicinal Plants*. 3(1), 16-24.

Karakaya, S., Göger, G., Bostanlik, F., Demirci, B., Duman, H., & Kilic, C. S. (2018). Comparison of the essential oils of Ferula orientalis L., Ferulago sandrasica Peşmen and Quézel, and Hippomarathrum microcarpum Petrov and their antimicrobial activity.

Turkish Journal of Pharmaceutical Sciences. 16(1), 69-89. https://doi.org/10.4274/tjps.77200

Kaur, M., Sharma, S., Kalia, A., & Sandhu, N. (2024). Essential oils and their blends: Mechanism of antibacterial activity and antibiofilm potential on food-grade maize starch packaging films. *International Microbiology*. 27(6), 1707-1724. https://doi.org/10.1007/s10123-024-00514-w

Keivanfar, L., Nateghi, L., Rashidi, L., & Pourahmad, R. (2025). Effect of Rosmarinus officinalis, Lavandula sublepidota, and Ferulago contracta essential oils on oxidative stability of camelina oil. *Journal of Food Quality.* 2025(1), 1781599. https://doi.org/10.1155/jfq/1781599

Kılıç, C. S., Catarino, I., Alves-Silva, J., Demirci, B., Kırcı, D., Salgueiro, L., & Zuzarte, M. (2025). Unlocking the skin-protective effects of ferulago spp. essential oils: A focus on antidermatophytic and wound-healing potential. *Antibiotics*. 14(4), 343-358. https://doi.org/10.3390/antibiotics14040343

Mashhadi-Sharif, N., Soodi, M., Mirnajafi-Zadeh, J., Shadboorestan, A., Ebadi-Ramsheh, H., & Bakhtiarzadeh, F. (2025). Ferulago angulata extract protects against beta-amyloid-induced memory impairment through modulation of monoaminoxidase enzymes in the rat's hippocampus. *Neurochemical Research*. 50(2), 1-15. https://doi.org/10.1007/s11064-025-04365-3

Moghaddam, M., Mehdizadeh, L., Mirzaei Najafgholi, H., & Ghasemi Pirbalouti, A. (2018). Chemical composition, antibacterial and antifungal activities of seed essential EO of F. angulata. *International Journal of Food Properties.* 21(1), 158-170. https://doi.org/10.1080/10942912.2018.1437626

Narimani, R., Moghaddam, M., Mahmoodi Sourestani, M., & Samiei, L. (2022). A comparative study on essential oil profile and antioxidant activity in different parts of three ferulago species. *Chemistry & Biodiversity*. 19(1), 202100513. https://doi.org/10.1002/cbdv.202100513

Nazzaro, F., Fratianni, F., D'Acierno, A., Coppola, R., Ayala-Zavala, F. J., Da Cruz, A. G., & De Feo, V. (2019). Essential oils and microbial communication. *In Essential Oils-Oils of Nature. IntechOpen*. https://doi.org/10.5772/intechopen.85638

Othman, R., Moarbes, V., Zaatar, M. T., Antonios, D., Roufayel, R., Beyrouthy, M., & Karam, M. (2025). Cytotoxic activity of essential oils from middle eastern medicinal plants on malignant keratinocytes. *Molecules.* 30(13), 2844-2860. https://doi.org/10.3390/molecules30132844

Phuong, H. N., Hien, N. T., Nguyen, Q. B., & Dinh, T. T. T. (2023). Chemical constituents of some essential EOs bearing plants growing wild in Vietnam. *Academia Journal of Biology*. 45(4), 83-92. https://doi.org/10.15625/2615-9023/18944

Pidlisnyuk, V., Newton, R. A., Ustak, S., Al Souki, K. S., Burdová, H., Trögl, J., & Mamirova, A. (2025). Assessing the potential of different biochars to support Miscanthus × giganteus phytoremediation in petroleum hydrocarbons-contaminated soil. *Industrial Crops and Products*. 229, 120971. https://doi.org/10.1016/j.indcrop.2025.120971

Rahanandeh, H., Sedaghatfar, E., Moshayedi, M., Nazari, N., & Chavoshi, S. (2024). In vitro evaluation of bio control agents and botanicals against mulberry root rot pathogen Fusarium oxysporum. *Journal of Organic Farming of Medicinal Plants.* 3(1), 44-49.

Sahu, A., Parai, D., Choudhary, H. R., & Singh, D. D. (2024). Essential EOs as alternative antimicrobials: current status. *Recent Advances in Anti-Infective Drug Discovery Formerly Recent Patents on Anti-Infective Drug Discovery.* 19(1), 56-72. https://doi.org/10.2174/2772434418666230316113927

Sharifi-Rad, J., Sureda, A., Tenore, G. C., Daglia, M., Sharifi-Rad, M., Valussi, M., & Iriti, M. (2017). Biological activities of essential oils: From plant chemoecology to traditional healing systems. *Molecules*. 22(1), 70-90. https://doi.org/10.3390/molecules22010070

Shavisi, N. (2024). Improving the oxidative stability of butter oil with nanoencapsulated Ferulago angulata essential oil during accelerated shelf-life storage. *Journal of Food Science and Technology.* 61(11), 2100-2110. https://doi.org/10.1007/s13197-024-05980-8

Shoeb, H. A., Madkour, H. M., Refahy, L. A., Mohamed, M. A., Saad, A. M., & Ghareeb, M. A. (2014). Antioxidant and cytotoxic activities of Gmelina arborea ROXB leaves. *British Journal of Pharmaceutical Research*. 4(1), 125-137. https://doi.org/10.9734/BJPR/2014/6018

Soares-Santos, R. R., Jaiswal, A. K., Ferreira, R. C. M., Azevedo, V. A. D. C., Aburjaile, F. F., & Soto-Blanco, B. (2025). Interactions of linalool and linalyl acetate with selected dog cytochrome p450 (CYP) proteins identified by in silico drug discovery followed by molecular docking analysis. *Pharmaceuticals.* 18(10), 1499-1510. https://doi.org/10.3390/ph18101499

Visan, A. I., & Negut, I. (2024). Coatings based on essential eos for combating antibiotic resistance. *Antibiotics.* 13(7), 625-637. https://doi.org/10.3390/antibiotics13070625

Wang, Y., Ma, J., Ma, C., Li, Z., Yin, S., Dai, J., & Ren, D. (2024). Antioxidant, antimicrobial and cytotoxic properties of Diospyros lotus L. essential oil with supercritical fluid extraction. *Journal of Food*

Measurement and Characterization. 18(5), 3236-3243. https://doi.org/10.1007/s11694-024-02398-w

Yeddes, W., Mejri, I., Grati, A. T., Khammassi, S., Hammami, M., Aidi, W. W., & Saidani, T. M. (2022). Synergistic effect of cloves (Syzygium aromaticum), thyme (Thymus vulgaris) and lemon (Citrus Limon) blended essential oils optimized by mixture design for improving the antioxidant activity. *Avicenna Journal of Medical Biochemistry.* 10(1), 20-29. https://doi.org/10.34172/ajmb.2022.03